

loading has 0 lobes, corresponding to the dread plane wave pattern in duct acoustics. Thus, it can be seen that running with an rpm differential gives direct diagnostic information otherwise not available by simple measurement methods.

It should be pointed out that a related diagnostic scheme was developed by Abdelhamid<sup>3</sup> in a ducted rotor experiment with simulated inlet guide vanes (IGV). He rotated the IGV assembly slowly to split the IGV interaction spectrum peaks from those due to other inflow disturbances.

The arguments presented above can be continued to higher harmonics with results shown in Fig. 2. In each BPF harmonic cluster, the highest and lowest peaks will be dominated by steady sources on the faster and slower rotors, respectively. Peaks in between are due to unsteady aerodynamic interaction.

### Conclusion

This mode-splitting behavior provides a powerful technique for noise source diagnosis in counter-rotation propellers and should be used in any noise tests where an rpm differential is possible.

### References

- <sup>1</sup>Hanson, D. B., "Noise of Counter-rotation Propellers," *Journal of Aircraft*, Vol. 22, July 1985, pp. 609-617.
- <sup>2</sup>Personal communication with Dr. Andrew Kempton of Rolls-Royce Acoustic Group, Oct. 16, 1984.
- <sup>3</sup>Abdelhamid, A. N., "Acoustic Response of a Model Ducted Rotor to Inflow Fluctuations," AIAA Paper 74-89, Jan. 1974.

## Stresses Around Holes in Pin-Loaded Orthotropic Plates

M.W. Hyer\*

University of Maryland, College Park, Maryland  
and

E.C. Klang†

University of Illinois, Champaign-Urbana, Illinois

### Introduction

IT was the purpose of the work reported herein to stay within the context of a two-dimensional analysis and study the effects of pin elasticity, clearance, and friction on the stress distributions around the hole in a pin-loaded orthotropic plate. The problem has direct application to the study of composite bolted joints and was studied for that purpose. The pin was considered as a second elastic body that interacted with the plate through contact. The pin, which exerts a net force on the hole edge, was represented by an elastic inclusion within the hole. In reality, the portions of the pin outside the thickness of the plate transmit, through shear, the load to the portion of the pin within the thickness of the plate.

Presented as Paper 84-0915 at the AIAA/ASME/ASCE/AHS 25th Structures, Structural Dynamics and Materials Conference, Palm Springs, CA, May 14-16, 1984; received June 4, 1984; revision submitted Aug. 13, 1985. Copyright © American Institute of Aeronautics and Astronautics, Inc., 1985. All rights reserved.

\*Professor, Department of Mechanical Engineering; formerly, Department of Engineering Science and Mechanics, Virginia Polytechnic Institute and State University, Blacksburg, VA. Associate Fellow AIAA.

†Research Associate, Department of Theoretical and Applied Mechanics.

In this study, since the shear stress across a cross-sectional area of the pin is nearly uniform, the effect of the shear stress was represented by a uniform in-plane body force acting on the elastic inclusion. With this two-dimensional approach, the pin elasticity being considered was an across-the-diameter elasticity. Complex variable elasticity, along with a numerical procedure, were used to find a solution to the problem. The numerical procedure consisted of collocation, to enforce the boundary conditions around the hole, and iteration, to find the contact and no-slip regions between the plate and pin. A complete discussion of the theory and the numerical procedure can be found in Ref. 1. With the analysis, the effects of pin modulus, friction levels, and degrees of clearance between the pin and plate could be assessed within the framework of the theory of elasticity. The problem was treated as a two-dimensional problem, as opposed to a three-dimensional one, to assess the effect of pin elasticity, friction, and clearance in the context of all the previous analyses that approached the problem as two-dimensional. With this approach, the seriousness of ignoring clearance, for example, in past analyses could be quantified. More importantly, composite bolted-joint design criteria based on a two-dimensional analysis and material failure data appear to give reasonable results when compared with test results.<sup>2</sup> Thus, a two-dimensional analysis has value. However, by using a two-dimensional approach, bolt-bending effects, clamping force (torque-up) effects, and interlaminar stresses cannot be accounted for.

### Numerical Results

Numerical results were computed in order to assess the effects of the various parameters on the stresses around the hole. The results reported on here are for a  $[0_2/\pm 45]_s$  graphite-epoxy laminate with the following material properties:

$$E_x = 85.5 \text{ GPa}, \quad E_y = 25.7 \text{ GPa}$$

$$G_{xy} = 22.1 \text{ GPa}, \quad \nu_{xy} = 0.667 \text{ GPa}$$

This represents a laminate with a moderate level of orthotropy,  $E_x:E_y = 3:1$ .

Figure 1 shows the effects of pin elasticity on the stresses around the hole edge. Three pin flexibilities are illustrated: a rigid pin ( $E = \infty$ ), a steel pin ( $E = 207 \text{ GPa}$ ), and an aluminum pin ( $E = 68.9 \text{ GPa}$ ). Poisson's ratio of the pin had very little effect on the numerical results. A value of 0.3 was used. Figure 1

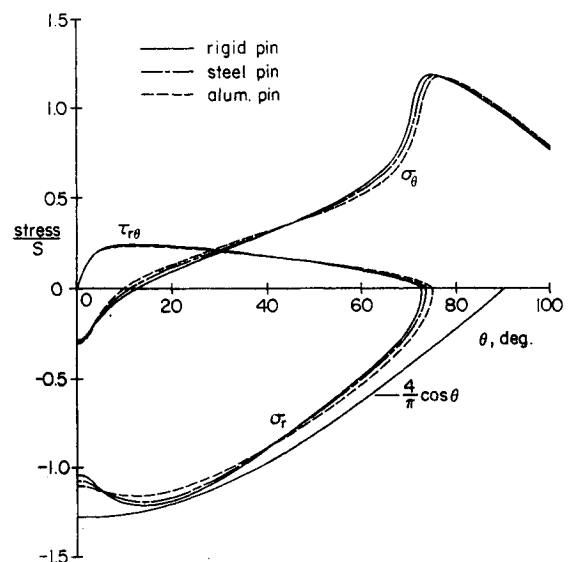


Fig. 1 Effect of pin elasticity on stresses around hole.

also shows the cosinusoidal radial stress distribution often assumed. Hence, Fig. 1 shows the two approximations, rigid and cosinusoidal, commonly used in this problem and in the situation studied here. The radial (bearing), friction-induced shear, and circumferential (hoop) stresses are shown in Fig. 1, and subsequent figures, as a function of circumferential position around the hole. The angle  $\theta=0$  deg coincides with the loading direction, and  $\theta=90$  deg is the net section. The stresses are nondimensionalized by the average bearing stress  $S$ . The bearing stress is defined as  $S=P/Dt$ , where  $P$  is the total load acting on the hole,  $D$  is the hole diameter, and  $t$  is the plate thickness. In computing the results of Fig. 1,  $\mu$  was chosen to be 0.2. This is a representative value for metal on graphite-epoxy. The clearance  $\lambda$  was 0.01 and the pin displacement  $\delta$  was 0.035. Since the hole radius was unity,  $\lambda$  and  $\delta$  should actually be thought of as nondimensionalized quantities, i.e.,  $\lambda/(\text{hole radius})$ , etc. Later figures will illustrate the effect of varying  $\mu$ ,  $\lambda$ , and  $\delta$ .

From Fig. 1 it is obvious that pin elasticity does not have a significant effect on the stress distribution around the hole. The cosinusoidal distribution is close, but it is not as accurate as the rigid pin assumption. While the rigid pin vs cosinusoidal distribution has been discussed in Ref. 3, no investigation to date has compared these two cases with an analysis that includes pin elasticity, friction, and clearance. The inaccuracy of

the cosinusoidal representation at  $\theta=90$  deg results from clearance effects, while its inaccuracy at  $\theta=0$  deg results from frictional effects. This will be illustrated below. Table 1 lists the contact and no-slip angles computed for the various situations, as well as the circumferential location of the maximum hoop and bearing stresses. The maximum hoop stress occurs very close to the end of the contact arc, while the maximum bearing stress occurs away from the centerline. The latter effect is also due to friction.

Figure 2 illustrates the effect of friction on the stresses at the hole edge. The results of Fig. 2 were computed using a steel pin with  $\lambda=0.01$  and  $\delta=0.035$ . As can be seen, friction decreases the bearing stress on the centerline and shifts the location of the maximum away from the centerline. Also, friction increases the maximum hoop stresses and changes the sign of the hoop stress at  $\theta=0$  deg. Such an effect was seen experimentally by Hyer and Liu.<sup>4,5</sup> As expected, the no-slip region increases with friction. The contact angle also increases and the location of the maximum hoop stress shifts slightly.

Finally, Fig. 3 illustrates the effect of clearance on the stresses around the hole edge. Here a steel pin with a friction coefficient of 0.2 and a displacement of 0.035 was used. The case of  $\lambda=0$  is a close-fitting pin and, for this case, the contact arc is only slightly less than 90 deg. As can be seen, clearance influences the contact arc and the maximum radial stress.

Table 1 Location of maximum hoop and radial stresses, contact, and no-slip regions for various cases

Fig. no.	Fixed conditions	Variable conditions	Location of max $\sigma_\theta$ , deg	Location of max $\sigma_r$ , deg	Contact arc $\beta$ , deg	No-slip arc $\alpha$ , deg
Pin						
1	$\mu = 0.2$	Rigid	74	14	73	$< 5$
	$\delta/R = 0.035$	Steel	75	14	74	$< 5$
	$\lambda/R = 0.01$	Aluminum	76	14	75	$< 5$
$\mu$						
2	Steel pin	0.0	77	0	71	—
	$\delta/R = 0.035$	0.2	75	14	74	$< 5$
	$\lambda/R = 0.01$	0.4	77	22	77	10
$\lambda/R$						
3	$\mu = 0.2$	0.00	86	13	86	$< 5$
	Steel pin	0.01	75	14	74	$< 5$
	$\delta/R = 0.035$	0.02	69	13	56	$< 5$

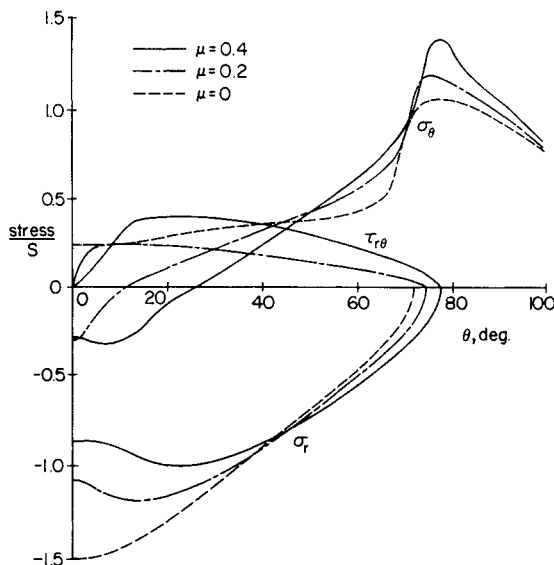


Fig. 2 Effect of friction on stresses around hole.

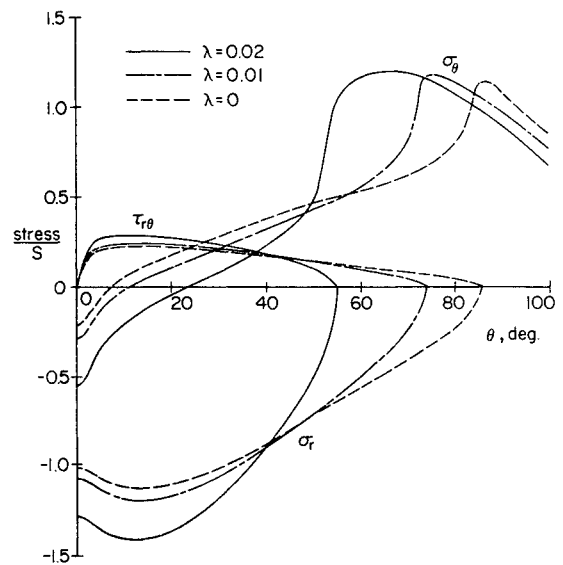


Fig. 3 Effect of pin/hole clearance on stresses around hole.

With less of a contact arc due to increased clearance, the radial stress has to be larger over the contact region to react the total load. The effect of clearance on the hoop stress is interesting. Even though the peak value is not influenced, the peak is spread over a larger circumferential region with increased clearance. With an increased volume of material at a high stress level, there is an increased likelihood of material failure. Also, with increased clearance, the region of maximum hoop stress moves toward  $\theta=0$  deg. It is expected that clearance levels would strongly influence where around the circumferential location damage or failure would occur in an actual joint.

### Concluding Remarks

From the results of this study, it can be concluded that pin elasticity is not an important variable. A rigid-pin assumption is accurate. The cosinusoidal assumption can be inaccurate. However, friction and clearance effects must be included in any realistic analysis.

### Acknowledgments

The work reported on here was supported by the NASA—Virginia Tech Composites Program, Cooperative Agreement NAG-1-343 with the NASA Langley Research Center.

### References

- <sup>1</sup>Hyer, M.W. and Klang, E.C. "Contact Stresses in Pin-Loaded Orthotropic Plates," *International Journal of Solids and Structures*, Vol. 21, No. 9, 1985, pp. 957-975.
- <sup>2</sup>Chang, F.K., Scott, R.A., and Springer, G.S., "Failure of Composite Laminates Containing Pin Loaded Holes-Method of Solution," *Journal of Composite Materials*, Vol. 18, No. 3, 1984, pp. 255-278.
- <sup>3</sup>Oplinger, D.W., "On the Structural Behavior of Mechanically Fastened Joints in Composite Structures," *Fibrous Composites in Structural Design*, edited by E.M. Lenoe, D.W. Oplinger, and J.J. Burke, Plenum Press, New York, 1980, pp. 575-602.
- <sup>4</sup>Hyer, M.W. and Liu, D., "Photoelastic Determination of Stresses in Multiple-Pin Connectors," *Experimental Mechanics*, Vol. 23, No. 3, 1983, pp. 249-256.
- <sup>5</sup>Hyer, M.W. and Liu, D., "Stresses in a Quasi-Isotropic Pin-Loaded Connector Using Photoelasticity," *Experimental Mechanics*, Vol. 24, No. 1, 1984, pp. 48-53.

## Impact of Loads Recording Methodology on Crack-Growth-Based Individual Aircraft Tracking

Robert M. Engle Jr.\*

*Flight Dynamics Laboratory  
Wright-Patterson Air Force Base, Ohio  
and*

*Thomas F. Christian Jr.†  
Damage Tolerance Analysis Laboratory  
Robins Air Force Base, Georgia*

### Introduction

SINCE its inception,<sup>1</sup> the Air Force Structural Integrity Program has used a fatigue analysis as the basis for its life calculations and the full-scale fatigue test to identify

"hot spots" and establish aircraft inspection intervals. The dominant parameter in any fatigue analysis is the magnitude of the loads. Hence, the recording devices chosen for aircraft tracking programs have historically been loads recorders. Counting accelerometers and multichannel (V-G-H) recorders have been used for years to collect loads data in terms of magnitude only.<sup>2</sup> V-G-H recorders measure velocity, load factor, and altitude. The Air Force is currently changing the individual aircraft tracking system from one based on fatigue to one based on fracture mechanics and crack growth. The fracture-mechanics-based crack growth analysis is much more sensitive to load sequence effects which lead to the crack growth retardation phenomenon. The transition to the crack-growth-based tracking programs gives rise to the question of whether the magnitude of the loads is a sufficient parameter for crack growth tracking. The objective of this study was to investigate the effects on crack growth life of various truncation patterns which simulate the manner in which certain typical tracking devices gather data. The baseline stress history chosen was a 200 flight sequence generated by the fighter aircraft loading standard for fatigue (FALSTAFF) program.<sup>3</sup> Two stress levels were evaluated. Analytical life predictions for all cases were performed using both fatigue and crack growth analyses. The sequences were then tested to determine experimental lives and the life variations were correlated.

### Experimental Procedure

The material used for this study was 2024-T3 aluminum. Test specimens were 4 in. wide  $\times$  16 in. long with a 0.25-in.-diam centered hole. All specimens were 0.25-in. thick. Crack growth specimens were precracked with a 0.02-in. radial through-crack on each side of the hole using the electrodischarge machining method. The fatigue specimens had no precrack. All testing was done in laboratory air. Each specimen was tested individually in a servocontrolled axial loading frame. The load sequences were programmed using a PDP 11/34 computer. Loading rate was 5 Hz. Crack lengths were measured using an optical microscope with an accuracy of 0.001 in.

### Stress Sequences

#### Baseline

The baseline stress sequence chosen was a 200 flight sequence generated using the FALSTAFF program. This 200 flight block contained 17,000 cycles in a random flight-by-flight sequence. The FALSTAFF sequence consists of integers from 0 to 32 that correspond to load levels determined by the input design limit stress.

#### V-G-H Simulation

Once the baseline sequence was obtained, an attempt was made to simulate the load magnitude data that would be obtained using a V-G-H recorder yet still retaining the sequencing information needed for a crack growth analysis. This was accomplished by filtering the 17,000-cycle baseline through 12 windows with a 1-g minimum threshold. The windows selected gave stress levels comparable to those on load/environment spectra survey (L/ESS) recorders on fighter aircraft. This gave a stress history that retained the sequence of the baseline FALSTAFF but was reduced from 32 to 12 levels and from 17,000 to 13,500 cycles.

#### Accelerometer Simulation

A similar filtering approach was taken to simulate a counting accelerometer while retaining sequencing information. The number of levels was adjusted to four, which is typical of the number of windows on a counting accelerometer. Again the minimum stresses were set to 1-g. Typical rise-fall criteria were applied to define the levels to be recognized. This truncation level gives the minimum information, reducing the 17,000-cycle baseline to 3550 cycles.

Presented as Paper 84-2410 at the AIAA/AHS/ASCE Aircraft Design Systems and Operations Meeting, San Diego, CA, Oct. 31-Nov. 2, 1984; received Nov. 20, 1984; revision received Sept. 6, 1985. This paper is declared a work of the U.S. Government and therefore is in the public domain.

\*Aerospace Engineer.

†Aerospace Engineer. Senior Member AIAA.